Sodium Decahydrido-*Closo*-1-Carbadecaborate as a Solid Electrolyte: New Insight into Polymorphism and Electrochemical Performance

Therese S. S. Kjær[1], Jakob B. Grinderslev[1], Lasse N. Skov[1], Torben R. Jensen[1]

Interdisciplinary Nanoscience Center (iNANO) and Department of Chemistry, Aarhus University, Langelandsgade 140, DK-8000 Aarhus C, Denmark

* Corresponding author: trj@chem.au.dk

Supporting Information

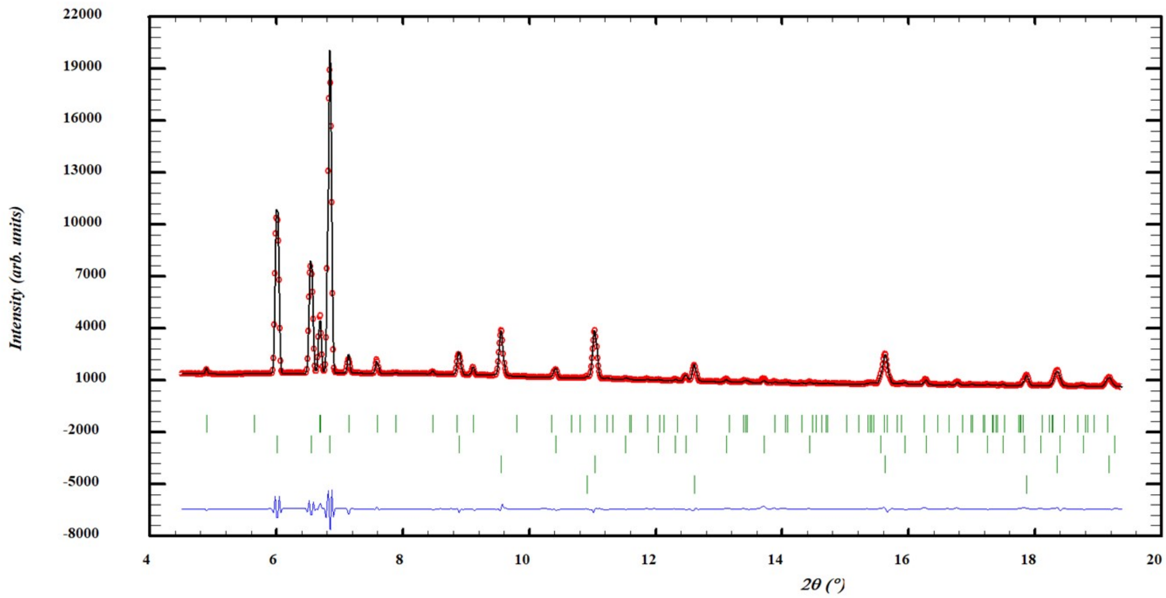

Figure S1. Rietveld refinement of SR-PXRD data of $NaCB_9H_{10}$ (**s1**) showing experimental (red circles) and calculated (black line) PXRD patterns, and a difference plot below (blue line) (T = 272 K, λ = 0.619689 Å). Green tick marks from top to bottom: *rt*-$NaCB_9H_{10}$, *ht*-$NaCB_9H_{10}$, NaI, NaCl. Final discrepancy factors: R_p = 2.25 %, R_{wp} = 3.57 % (not corrected for background), R_p = 10.5 %, R_{wp} = 9.54 % (conventional Rietveld R-factors). Mass fractions: *rt*-$NaCB_9H_{10}$ (22.4 wt%), *ht*-$NaCB_9H_{10}$ (69.7 wt%), NaI (4.8 wt%) and NaCl (3.1 wt%).

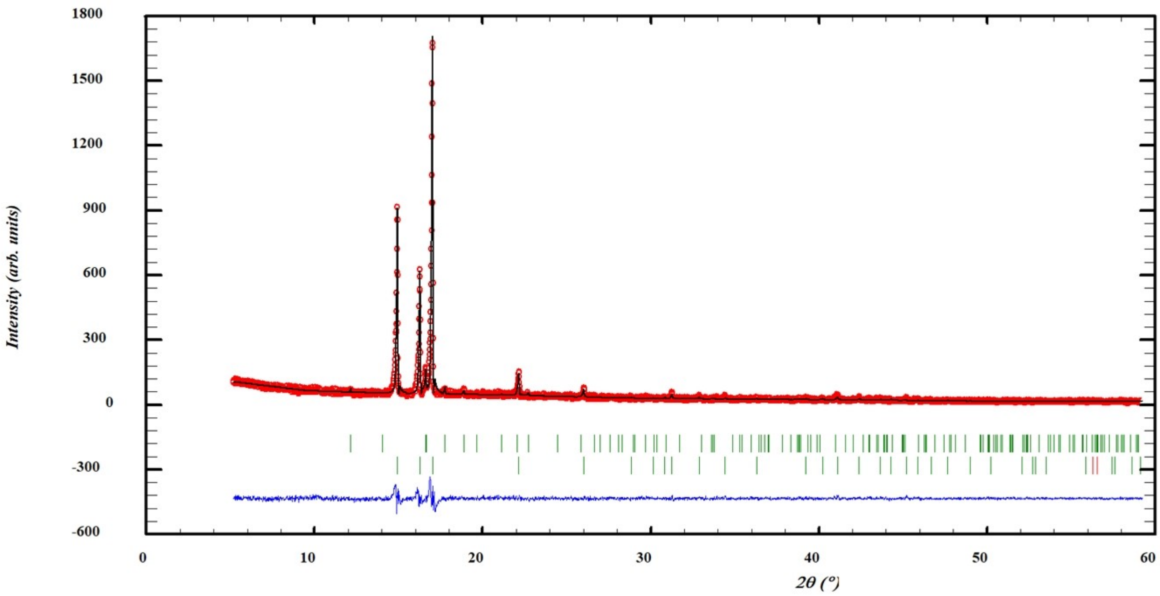

Figure S2. Rietveld refinement of PXRD data of as-synthesized *ht*-$NaCB_9H_{10}$ (**s2**) showing experimental (red circles) and calculated (black line) PXRD patterns, and a difference plot below (blue line) (T = 294 K, λ = 1.5405 Å). Green tick marks from top to bottom: *rt*-$NaCB_9H_{10}$, *ht*-$NaCB_9H_{10}$. Final discrepancy factors: R_p = 10.9 %, R_{wp} = 9.60 % (not corrected for background), R_p = 46.8 %, R_{wp} = 11.2 % (conventional Rietveld R-factors). Mass fractions: *rt*-$NaCB_9H_{10}$ (12.0 wt%), *ht*-$NaCB_9H_{10}$ (88.0 wt%).

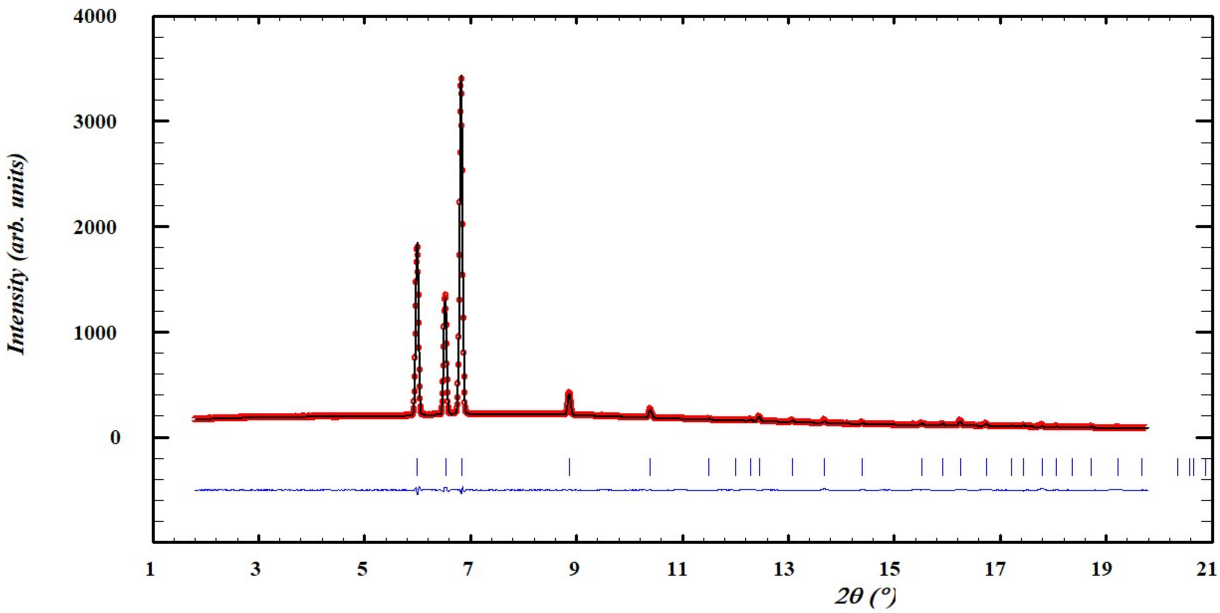

Figure S3. Rietveld refinement of SR-PXRD data of *ht*-$NaCB_9H_{10}$ (**s2**) showing experimental (red circles) and calculated (black line) PXRD patterns, and a difference plot below (blue line) (T = 294 K, λ = 0.6199 Å). Blue tick marks: *ht*-$NaCB_9H_{10}$. Final discrepancy factors: R_p = 0.859 %, R_{wp} = 1.47 % (not corrected for background), R_p = 4.37 %, R_{wp} = 4.28 % (conventional Rietveld R-factors), R_{Bragg}(*ht*-$NaCB_9H_{10}$) = 1.63 % and global χ^2 = 83.8.

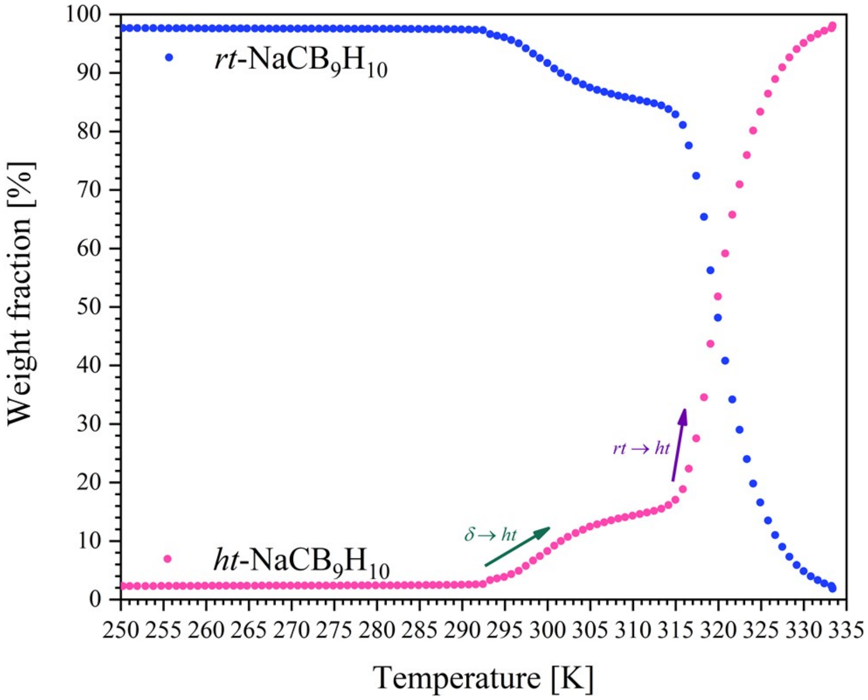

Figure S4. Relative weight fractions of crystalline *rt*- (blue) and *ht*-$NaCB_9H_{10}$ (pink) is extracted by Rietveld refinement of SR-PXD data measured of $NaCB_9H_{10}$ (**s1**) during the initial heating, see Figure 2 ($\Delta T/\Delta t$ = 5 K min^{-1}). The amount of δ-$NaCB_9H_{10}$ in the sample is estimated to 12.8 wt% and used to rescale the fraction of crystalline material. The green arrow marks the initiation of the formation of crystalline *ht*-$NaCB_9H_{10}$ from δ-$NaCB_9H_{10}$, the purple arrow marks the initiation of the polymorphic transition from *rt*- to *ht*-$NaCB_9H_{10}$.

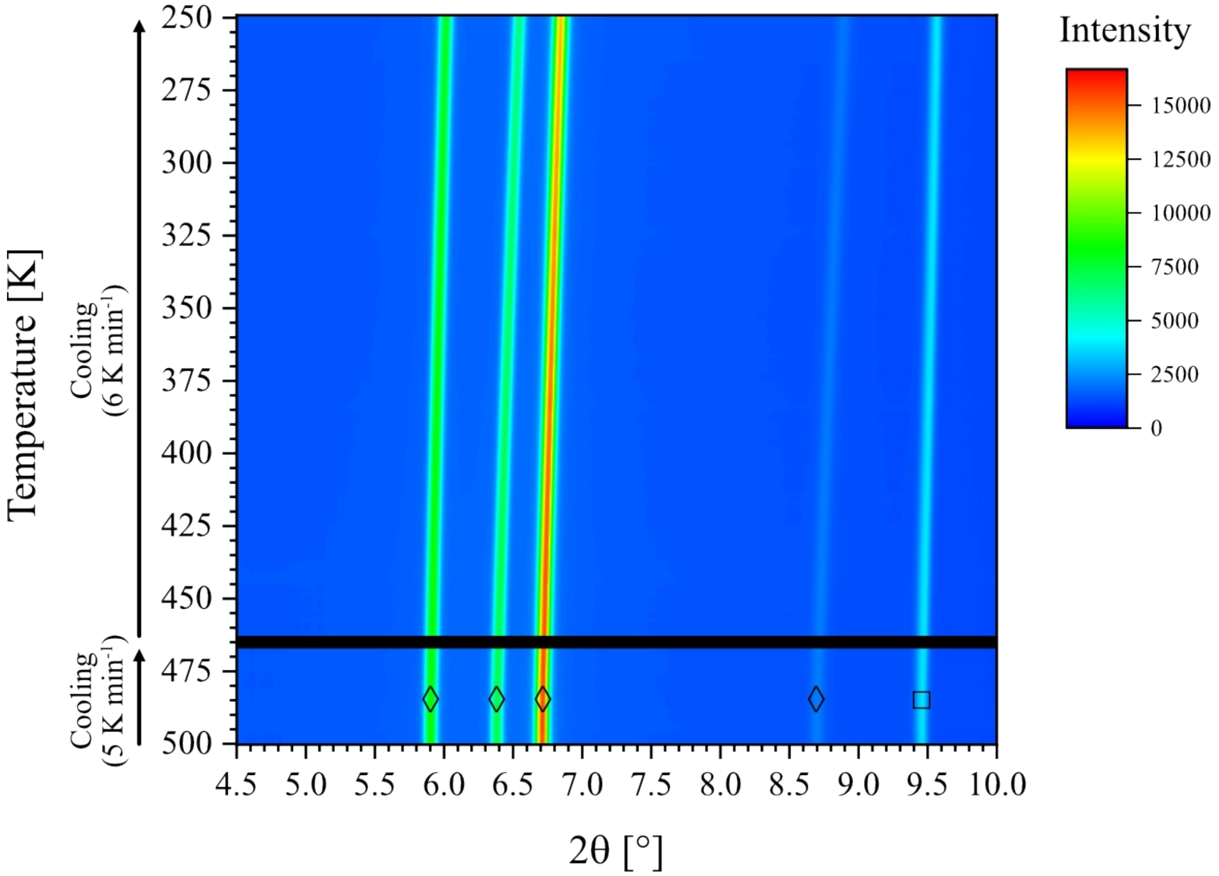

Figure S5. *In situ* SR-PXRD of the subsequent cooling of $NaCB_9H_{10}$ (**s1**), i.e. a continuation of the diffraction experiment shown in Figure 2 (λ = 0.619689 Å, $\Delta T/\Delta t$ = 5 K min^{-1} from 500 to 467 K, and $\Delta T/\Delta t$ = 6 K min^{-1} from 463 to 250 K). Symbols: *ht*-$NaCB_9H_{10}$ (◊), NaI (□).

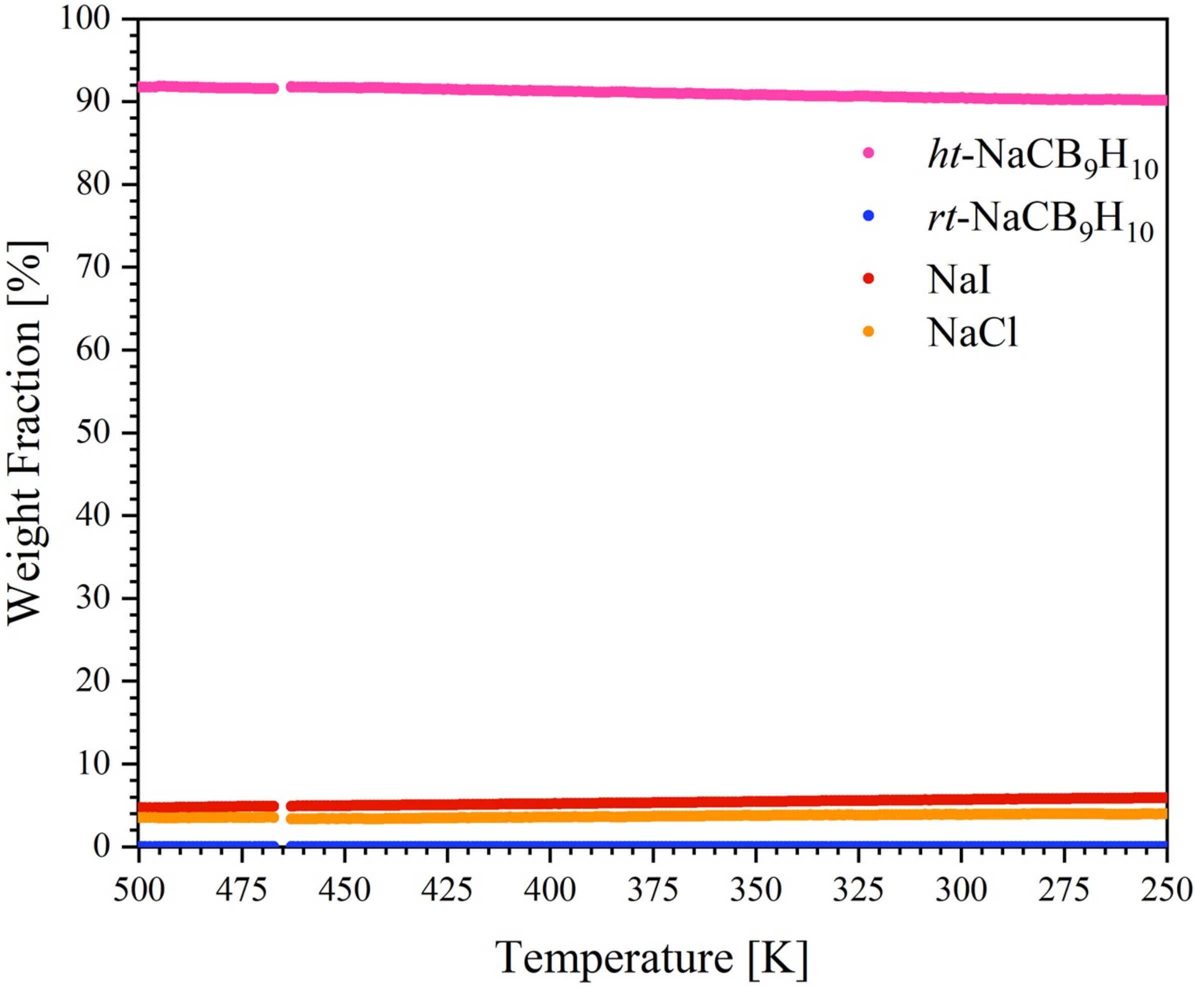

Figure S6. Crystalline weight fraction of *rt*- (blue), *ht*-$NaCB_9H_{10}$ (pink), NaI (red) and NaCl (orange) extracted by Rietveld refinement of SR-PXRD data (shown in Figure S4).

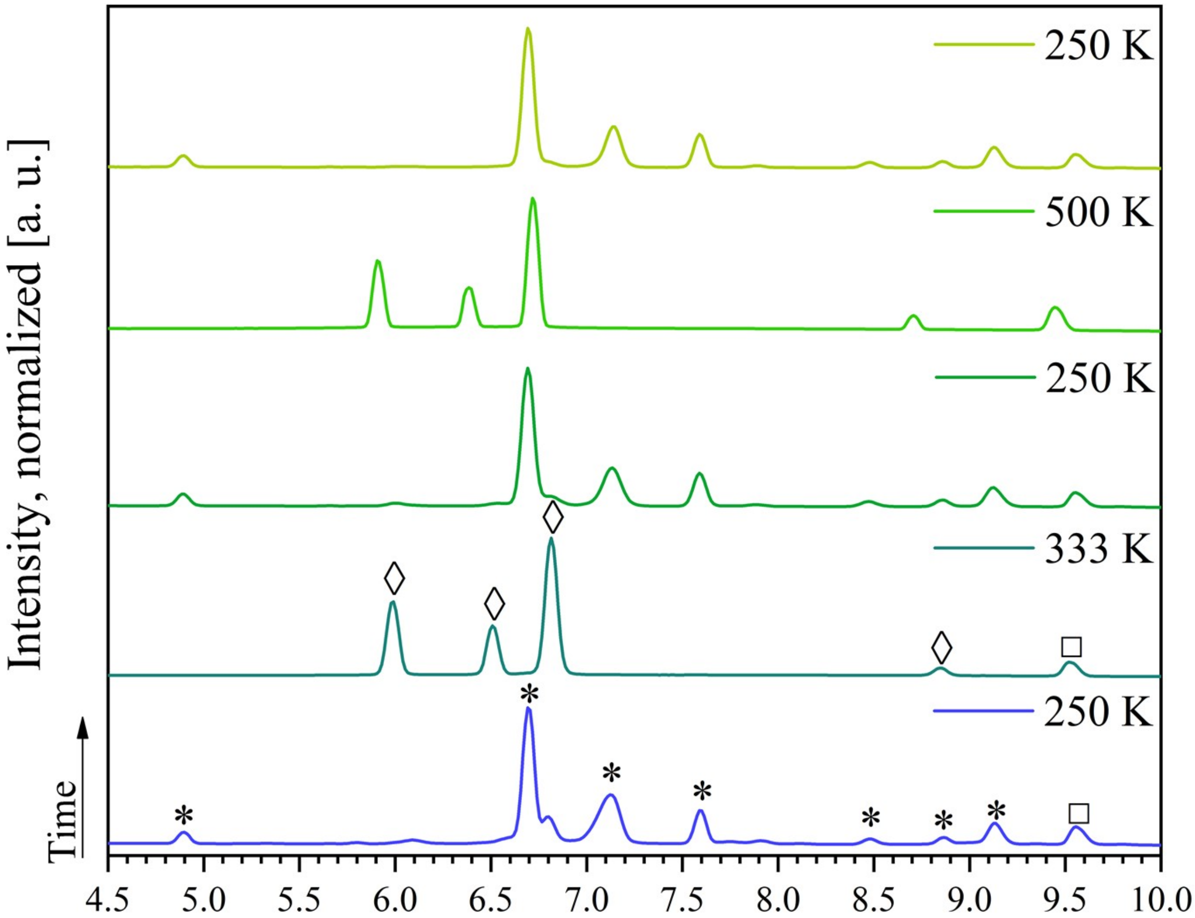

Figure S7. SR-PXRD of $NaCB_9H_{10}$ (**s1**) (λ = 0.619689 Å) at different temperatures. This sample was used for the measurement shown in Figure 2, however the capillary was moved such that a "new" spot on the sample was exposed to the X-rays. Symbols: *rt*-$NaCB_9H_{10}$ (*), *ht*-$NaCB_9H_{10}$ (◊), NaI (□).

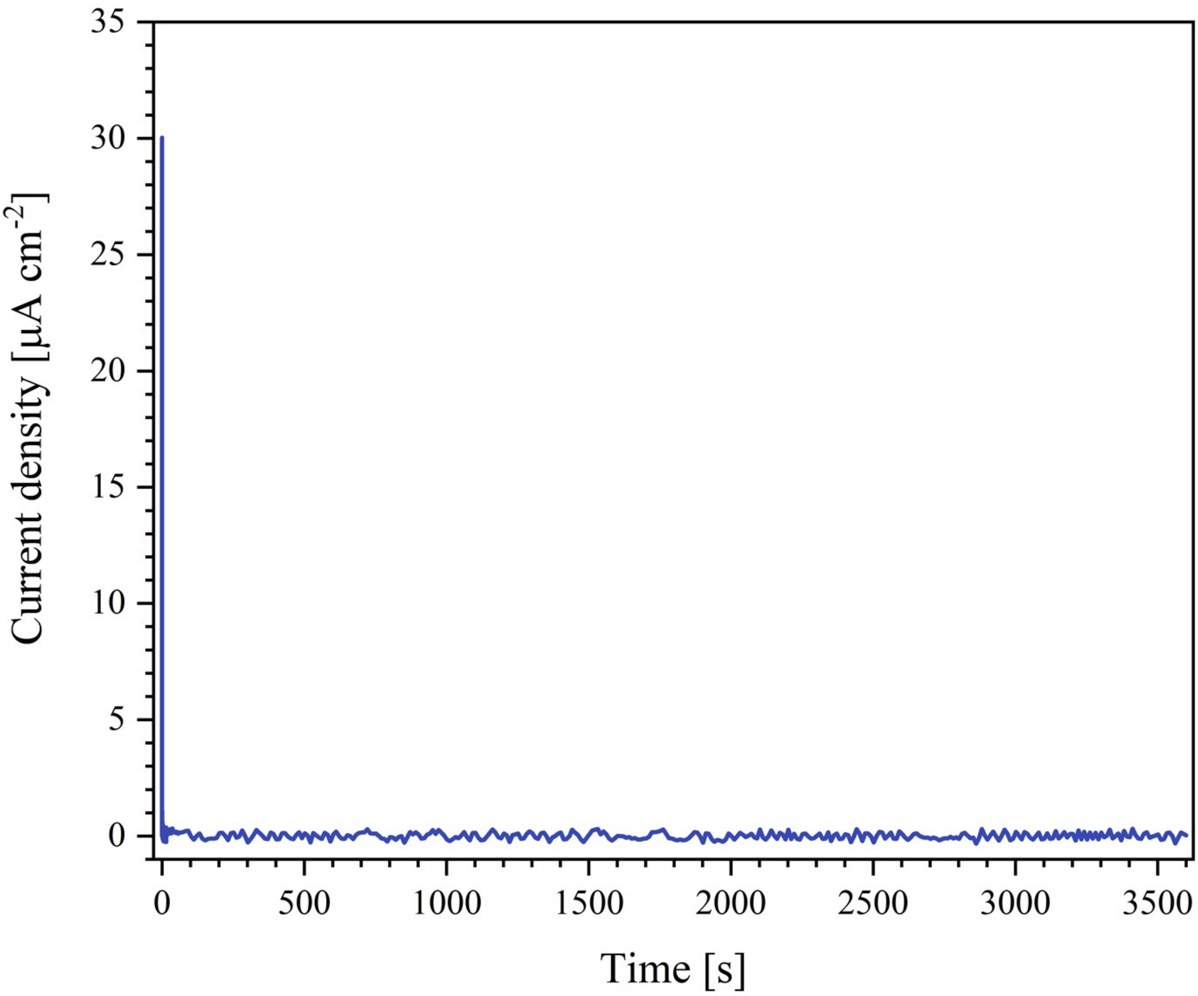

Figure S8. A symmetric SS|$NaCB_9H_{10}$ (**s2**)|SS cell to determine the ionic transport number, t_{ion}.

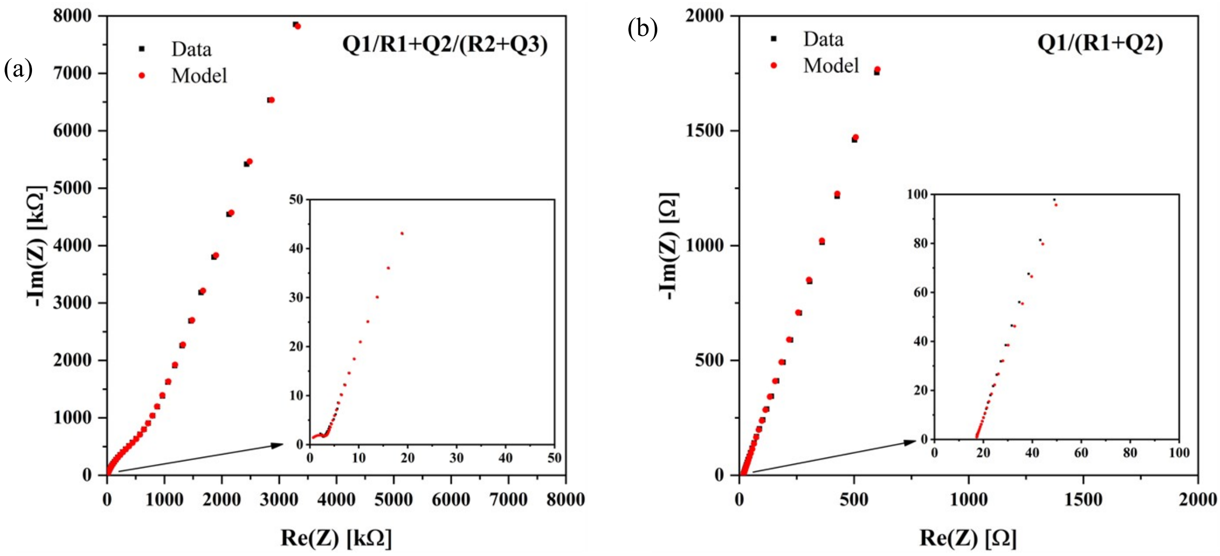

Figure S9. Nyquist plots and the corresponding equivalent circuit fits of $NaCB_9H_{10}$ (**s1**) measured at room temperature before heating (a) and after the first heating cycle (b). The data before heating displays two semicircles, attributed to the presence of both *rt*-$NaCB_9H_{10}$ and *ht*-$NaCB_9H_{10}$ in the as-synthesized sample. Only a single conducting phase is present after the initial phase transition to *ht*-$NaCB_9H_{10}$ at T > 333 K and the semicircle is no longer observed due to the low resistance in *ht*-$NaCB_9H_{10}$.

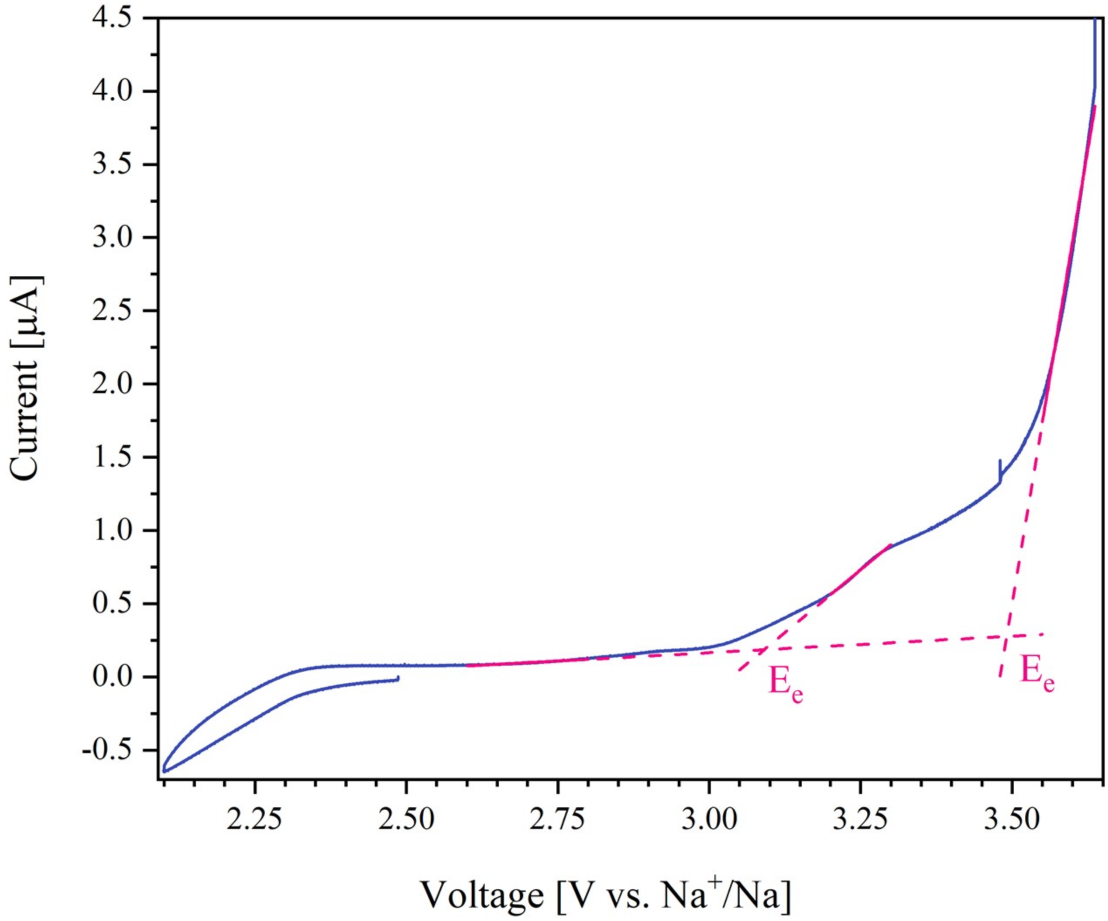

Figure S10. Linear sweep voltammetry showed two anodic peaks for $NaCB_9H_{10}$ (**s2**), one with an edge potential of 3.1 V and a larger peak with an edge potential of 3.5 V. At 3.6 V the current increased rapidly skewing the edge potential to a larger value if included.

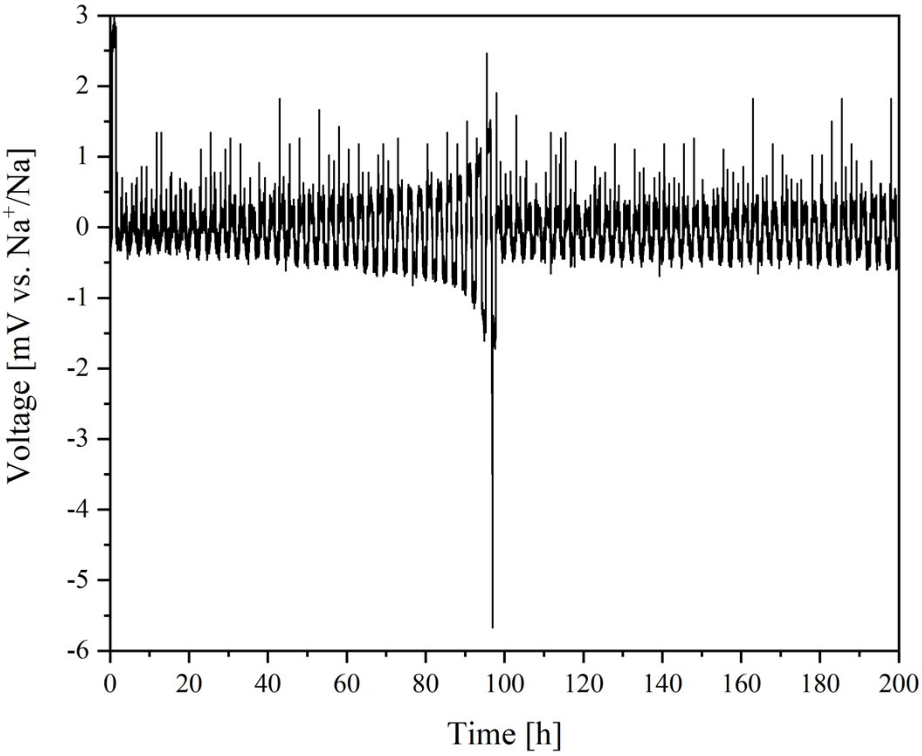

Figure S11. Precycling of Na|$NaCB_9H_{10}$ (s**1**)|Na cell used for critical current density measurement conducted at T = 303 K and 0.2 mA cm^{-2} for 80 cycles.

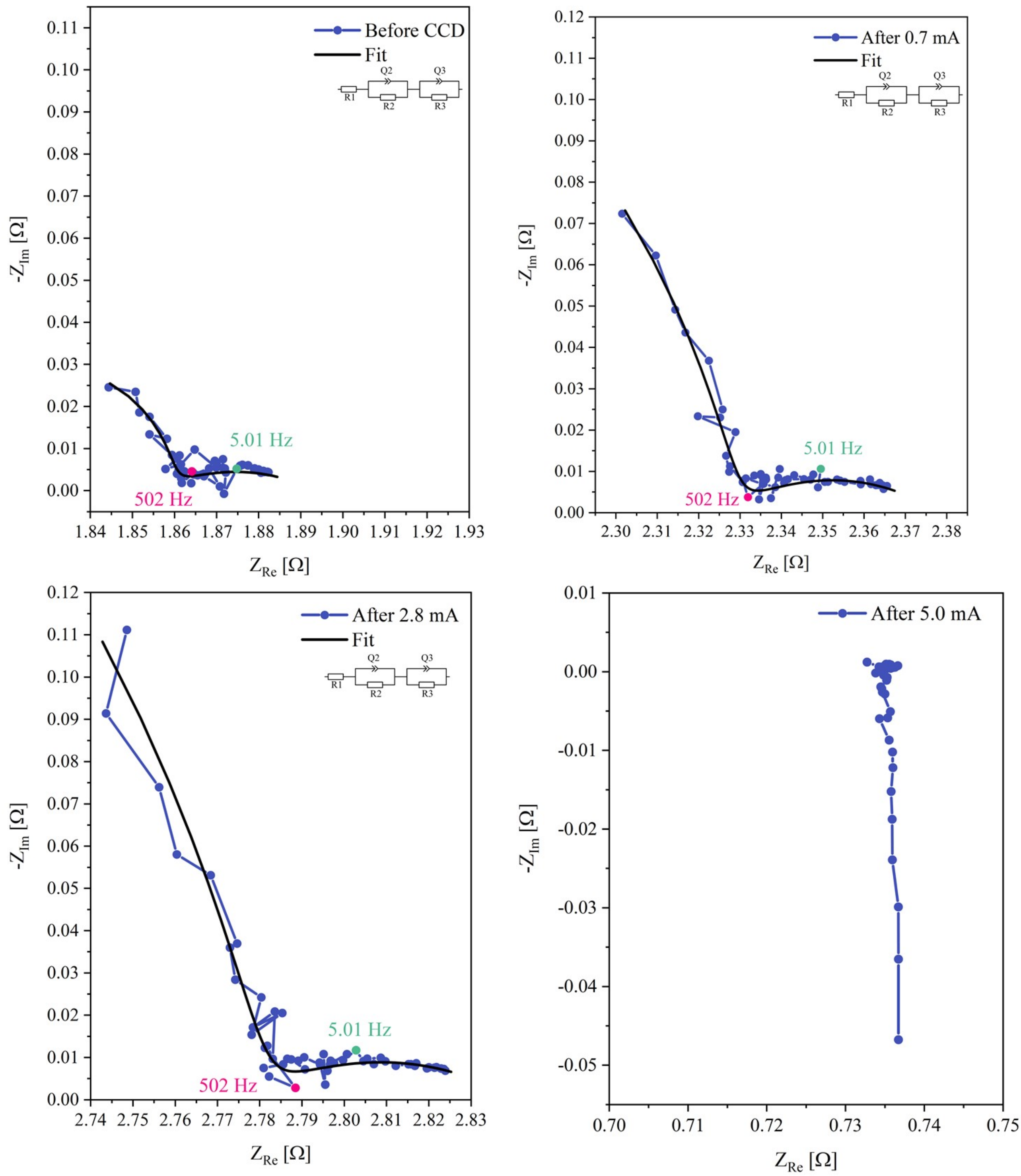

Figure S12. Nyquist plot of EIS measurements throughout the investigation of critical current density, raw data (blue) fitted (black) with R1+Q2/R2+Q3/R3. R1 is ascribed as the internal resistance of the cell, R2 is associated with the interface between the solid electrolyte and the electrodes, R3 is ascribed as a low frequency resistance.

Tabel S1. Fitted resistance from Nyquist plot of EIS measurements (Figure S9) throughout the investigation of critical current density.

	Before CCD [Ω]	After 0.7 mA [Ω]	After 2.8 mA [Ω]
R1	1.799	1.914	2.029
R2	0.05659	0.4126	0.7481
R3	0.03714	0.05091	0.06319